AFOSR-TR-97-0407

REPORT DOCUMENTATION PAGE

Form Approved
OMB No. 0704-0188

1. AGENCY USE ONLY (Leave blank)	2. REPORT DATE	3. REPORT TYPE AND DATES COVERED
	September1, 1997	Final Report 6/14/94-6/14/97

4. TITLE AND SUBTITLE

INTEGRATED POLYMER-SEMICON DUCTOR OPTO-ELECTRON ICS: BASIC MATERIALS STUDIES

5. FUNDING NUMBERS

Award number
F49620-94-1-0323

1651/01

62173C

6. AUTHORS

Dr. William Steier

7. PERFORMING ORGANIZATION NAME(S) AND ADDRESS(ES)

University of Southern California
Department of Engineering/Electro-Physics
Los Angeles, California 90089/0483

8. PERFORMING ORGANIZATION

9. SPONSORING/MONITORING AGENCY NAMES(S) AND ADDRESS(ES)

Dr. Charles Y-C Lee
Directorate of Chemistry and Materials Science
Air Force Office of Scientific Research
Bolling Air Force Base, DC 20332-6448

10. SPONSORING/MONITORING AGENCY REPORT NUMBER

11. SUPPLEMENTARY NOTES

DISTRIBUTION STATEMENT A
Approved for public release
Distribution Unlimited

12a. DISTRIBUTION/AVAILABILTY STATEMENT

release, distribution unlimited

12b. DISTRIBUTION CODE

13. ABSTRACT (Maximum 200 words)

The objective of this research is to bring the demonstrated advantages of the electrooptic polymers into use in photonic devices and systems. In this report we demonstrate a waveguide taper section for improved mode matching between the traveling wave electrooptic polymer modulator and input and output fibers. The taper section increases the waveguide mode and reduces the fiber coupling loss at each end by approximately 2 dB. The design is compatible with current modulator design. We also report on a polymer bleaching process for balancing the outputs of a waveguide Y junction. This process is used to increase the extinction ratio of a polymer Mach Zehnder modulator.

14. SUBJECT TERMS

Electroopic polymers, Optical Modulation, Optical waveguides

15. NUMBER OF PAGES

24

16. PRICE CODE

17. SECURITY CLASSIFICATION of report	18. SECURITY CLASSIFICATION of this page	19. SECURITY CLASSIFICATION of abstract	20. LIMITATION OF ABSTRACT

UNIVERSITY OF SOUTHERN CALIFORNIA

SCHOOL OF ENGINEERING

INTEGRATED POLYMER-SEMICONDUCTOR OPTO-ELECTRONICS: BASIC MATERIALS STUDIES

F49620-94-1-0323

Final Report
September 1, 1997

Submitted to:

Dr. Charles Y-C Lee

Directorate of Chemistry and Materials Science
Air Force Office of Scientific Research
Bolling Air Force Base, DC 20332-6448

Submitted by:

William H. Steier,
Professor of Electrical Engineering
School of Engineering

University of Southern California
Los Angeles, California 90089-0483

UNIVERSITY OF SOUTHERN CALIFORNIA

MATERIALS AND FABRICATION STUDIES FOR ADVANCED POLYMER ELECTRO-OPTIC DEVICES
F49620-94-1-0323

Final Report
9/1/97

Submitted to:
DR. CHARLES Y-C LEE
DIRECTORATE OF CHEMISTRY AND MATERIALS
AIR FORCE OFFICE OF SCIENTIFIC RESEARCH
BOLLING AIR FORCE BASE, DC 20332-6448

Submitted by:
WILLIAM H. STEIER
UNIVERSITY OF SOUTHERN CALIFORNIA
LOS ANGELES, CA 90089-0483
Tele: 213 740 4415
FAX: 213 740 8684
e-mail: steier@mizar.usc.edu

I. Introduction and Research Objective

The objective of this research is to bring the demonstrated advantages of the electrooptic polymers into use in photonic devices and systems. The recent dramatic advances in these materials in terms of their EO coefficients, thermal stability, and in the fabrication of low loss optical waveguides make them prime candidates for high speed optical switches and modulators. The objective is therefore to develop fabrication strategies, prototype device designs, and packaging techniques for high speed polymer electrooptic devices and to demonstrate the feasibility of on chip integration of polymer EO switches with high speed semiconductor electronics. An additional goal is to support the EO polymer synthesis research, under the direction of Professor L. R. Dalton in the Chemistry Department at USC, with optical and EO materials measurements.

II. Integrated Optical Mode Taper - Reduction of Insertion Loss

The insertion loss of an optical waveguide device packaged with optical fibers comes from two major sources: fiber coupling loss and the propagation loss in the waveguide. At the telecommunication wavelength of 1.3 μm, the propagation loss is approximately 0.4 dB/cm for passive polymers and 1 dB/cm for electrooptic polymers . The coupling loss between a typical single mode polymer channel waveguide and a standard single mode silica fiber is typically 4-6 dB per connection. Most devices are 1-3 cm long, and fiber coupling loss is the dominant part of device insertion loss. Therefore fiber coupling loss has to be minimized to reduce the device insertion loss. The largest part of the coupling loss comes from the mode mismatch between optical fiber and waveguide, similar to the situation of fiber coupling with semiconductor optoelectronic devices. The circular mode of a standard 1.3 μm single mode fiber is typically 10 μm in diameter; a typical polymer waveguide mode is a 5 μm (lateral) by 1-2 μm (vertical) ellipse. The difference in size and shape between the two modes makes the coupling between fiber and waveguide inefficient.

Because of restrictions on the total thickness of waveguide layers to keep $V\pi$ low, it is not practical to make single mode waveguide with a large mode size by simultaneously increasing the core layer thickness and reducing the index difference between core and cladding. We describe a unique taper mode size transformer to improve coupling between single mode channel waveguides and standard single mode fiber. Our approach can keep the waveguide structure optimized for device function, and uses independent transformer sections integrated at the ends of device chip to expand the mode size. The taper transformer also brings about an additional benefit of increasing fiber misalignment tolerance.

The design and fabrication of tapers in polymer waveguides can be very different from those with semiconductor optoelectronic devices. A lateral taper, which works well with semiconductor lasers and amplifiers and which is easy to fabricate with regular photolithography and etching, is not very useful with polymer waveguides because the mode mismatch between a polymer waveguide and fiber is mainly in the vertical direction. A vertical taper is

necessary to expand the mode in that direction. Another structure often used with semiconductor optoelectronic devices, the down tapering of waveguide core, is also not suitable for polymer waveguides. The down taper produces a mode larger than the few μm of cladding width. Light will suffer high propagation loss if the evanescent tails penetrate into the metal electrodes and substrate. Moreover, down tapering of the core layer requires strict control of layer thickness because the final thickness of the waveguide after etching is only tens of nanometers. This extremely small thickness is comparable to even the thickness variation of spin-cast polymer films if the film is a few micrometers thick. On the other hand, polymers offer a wide range of refractive index from which to choose. They can be thermoset, thermoplastic, and photoprocessible.

We present here a vertically tapered mode size transformer integrated with polymer channel waveguides. The processing of this mode size transformer is performed on the already processed waveguide devices and is independent of previous device processing steps. A vertical taper is made in the upper cladding of the waveguide with simple masked reactive ion etching (RIE) techniques. The etched area is subsequently covered by a new cladding of higher index material. We will first analyze the principles of this taper transformer, followed by a description of the fabrication procedures, especially taper etching techniques. Finally, experiment results of mode expansion, increase of fiber misalignment tolerances, and reduction in coupling loss with standard 1.3 μm single mode fiber of 10 μm mode size are demonstrated. This approach of mode size transformer is not designed for perfect mode match, yet it is a simple method to achieve a considerable reduction in fiber coupling loss.

A. The Concept

Our proposed mode size transformer is based on the most common structure of polymer waveguide devices , as shown in Fig. 1. The waveguide is a tri-layer structure consists of a lower cladding, a core layer patterned with channel waveguides, and an upper cladding. The typical thickness of the core layer is 1-2 μm and the thickness of cladding layers is 4-5 μm. In the cases of waveguide modulators and switches, metal electrodes are made either under the lower cladding or also on top of upper cladding. Because metal electrodes and some substrates strongly absorb light, to expand the vertical dimension of the mode without introducing extra propagation loss due to such absorption, the mode should only grow upward, in the area where the top electrode in not present. Fig. 2 illustrates our proposed vertically tapered mode size transformer for this purpose. The transformer is fabricated on an device chip with waveguides and electrodes already made. No change of previous device fabrication steps is needed. The upper cladding near the end of the chip tapers off and the core layer is exposed. Then a new cladding with higher index than the removed upper cladding is put on the etched area. Since the index difference between this new cladding and the core layer is smaller, the mode is more weakly confined from the top. As light propagates along the taper, mode size gradually grows in that direction. The confinement by the lower cladding is not affected. Therefore no additional propagation loss is introduced because the mode does not expand toward metal and lossy substrate. The lateral

confinement is also very little affected because the change of the effective index difference in the lateral direction is negligible. The transformed mode is bigger and more circular, and it matches better with fiber mode.

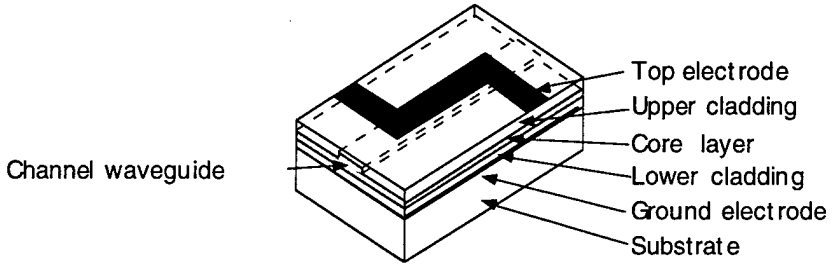

Fig. 1 Structure of a typical polymer waveguide device. The length of the device is not draw to scale.

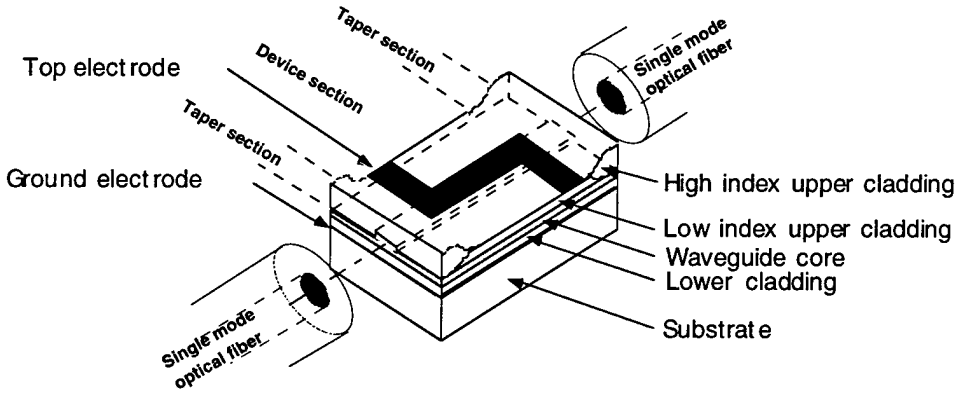

Fig. 2 A schematic diagram of the proposed mode size transformer with vertical taper for fiber coupling. The length of the device is not draw to scale.

For a smooth mode size transition and to minimize radiation losses, the taper should be long enough so that the maximum taper slope is less than the critical slope for the adiabatic condition . The process of the mode transformation and simulated mode profiles in different stages of mode transformation is shown in Fig. 3. The simulation is made with Fwave IV, a freeware for waveguide mode calculation. An adaptive vectorial finite difference method was used to calculate local modes in the taper, and the results were verified with Fourier decomposition method.

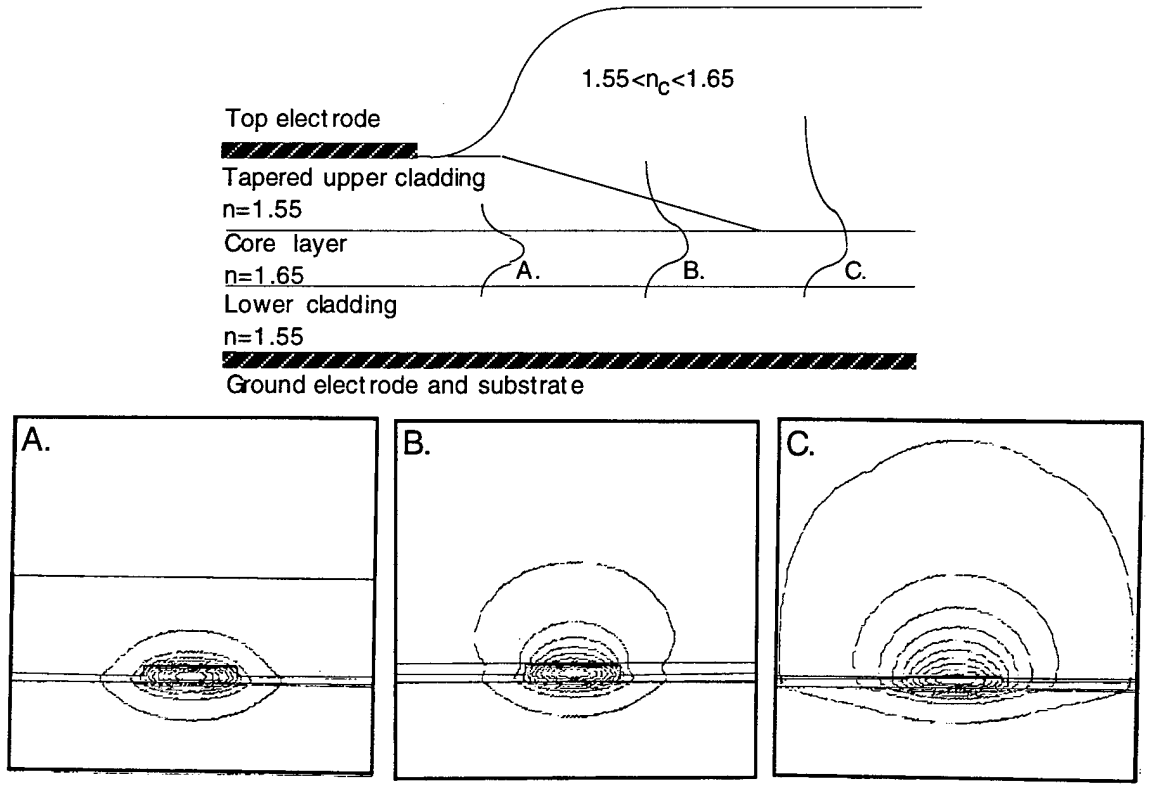

Fig. 3 Mode expansion in the taper section. The outmost contour line is 1% of the peak electric field, and the rest lines are 10-90% of the peak, in 10% increment. The same assignment of contour lines is used in Fig. 4.

The degree of mode expansion depends on the refractive index of the new cladding. Fig. 4 shows the modes of a ridge waveguide with various new cladding indices. Higher index makes the mode bigger. However, beam propagation simulation indicates that if the new cladding index is higher than the effective index of the waveguide before the taper section, higher radiation loss in the taper may occur. Therefore we limited our new cladding index below the waveguide effective index in our experiments.

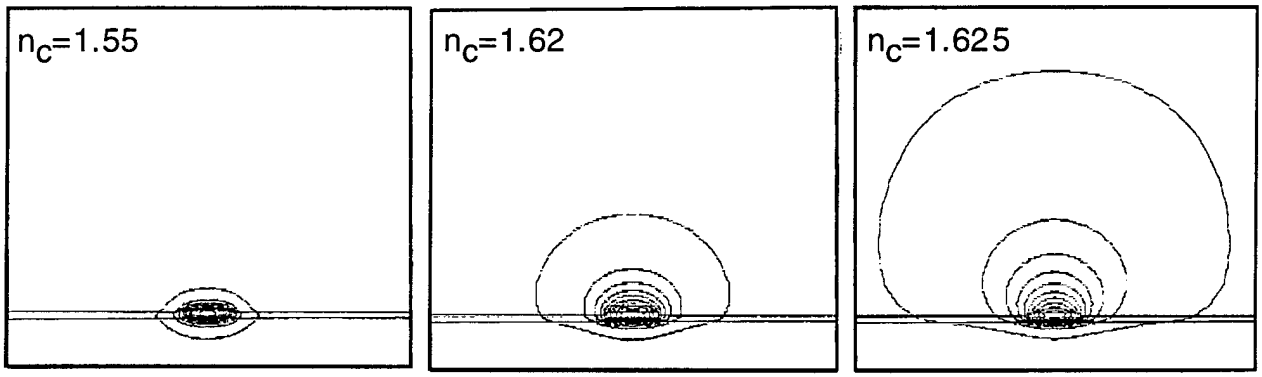

Fig. 4 Simulation results of transformed modes with various new cladding indices.

The thickness of the new upper cladding should be thick enough to contain the mode tail. This condition is the only requirement on the thickness of the new cladding because there is no restriction on its maximum thickness. No precise film thickness control is needed. This property is very desirable in device fabrication. Also our structure is not as sensitive to etch depth as the down taper in semiconductor waveguides, because the final thickness of the core layer after etching is still at least an order of magnitude thicker.

The lowest coupling loss this mode size transformer can achieve is limited by the asymmetric nature of the expanded mode in the vertical direction. In that direction the expanded mode approaches an exponential function. The minimum coupling loss due to mode mismatch in vertical direction is estimated using overlapping integral, and the result is approximately 1 dB. The lateral distribution of the expanded mode matches well with a Gaussian function. The lateral size of the mode can also be easily adjusted by changing the width of the waveguide. The coupling loss due to lateral mismatch is usually found to be less than 0.1 dB. For a practical device coupled with standard single mode fiber of 10 μm mode size, a coupling loss as low as 1.5-2 dB is predicted in theory. This value is 2-4 dB lower than coupling without the tapered mode size transformer. Coupling loss less that 1 dB is achievable with a fiber that has smaller (6.3 μm) mode.

B. Fabrication

The taper is fabricated in two steps: taper etching and coating of new cladding. They are done as the last processing steps of the entire device. Two different masked RIE techniques have been used to make the vertical taper and both techniques were effective.

RIE with shadow mask The first method we describe is oxygen RIE with a shadow mask, as illustrated in Fig. 5.

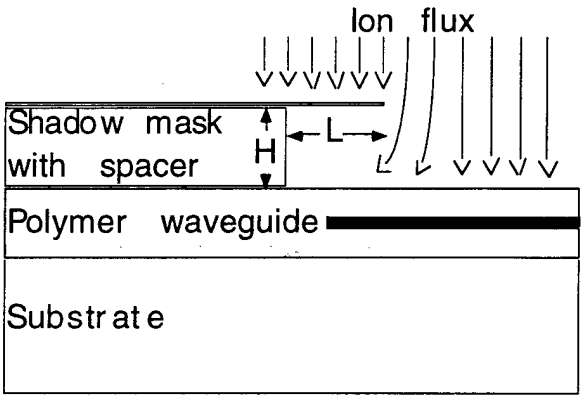

Fig. 5 Taper etching with a shadow mask in oxygen plasma.

The shadow mask is a 0.25 mm glass slide. It is attached with UV epoxy to a glass spacer which supports the shadow mask and defines the height of the shadow mask. The mask is placed on the sample and etching is carried out in a standard parallel plate (Plasma Technology Plasmalab) etcher at a pressure of 400 mTorr, rf power of 40 W, and 50 sccm O_2 flow rate. The shadow mask partially shields the sample underneath and also deflects the ion flux, causing a position dependent etch rate in the vicinity of the end of the shadow mask. An example of measured surface profile of an etched taper is given in Fig. 6a. The taper has a smooth S-shape and fits well into function

$$y = \frac{h}{1 + e^{8\frac{x-c}{l}}} + d,$$

where parameters l, h, c and d are defined in Fig. 6b.

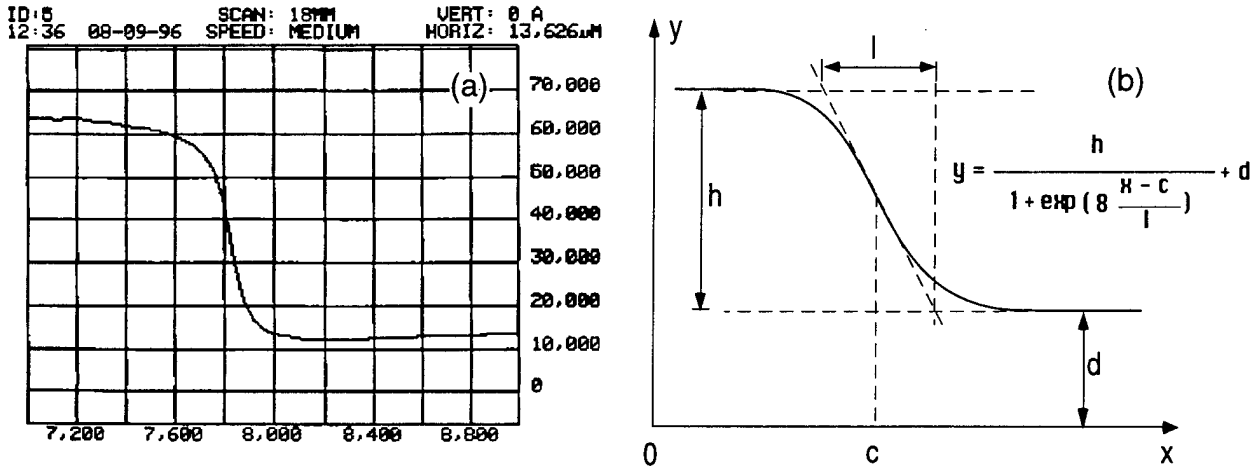

Fig 6 (a) A surface profile of a taper etched with shadow mask RIE. The horizontal scale is in µm and the vertical scale is in Å. (b) Function used for fitting the taper. l: taper length; h: etch depth; c: taper center; d: final thickness of the film.

For a given RIE condition, the length of the taper, l, is determined by the height of the shadow mask, as shown in Fig. 7. l is independent of the length L of the shadow mask as long as L is larger than 2 mm. An interesting phenomenon is that the taper length does not change during etching. Fig. 8 shows l and h as functions of etching time. The etch depth is linearly proportional to etching time due to a constant etch rate. As the result of a constant l and linear increase of h, the maximum slope of the taper increases linearly with time. The shape of the taper is found to be quite insensitive to the change in etching parameters.

We also experimented with metal shadow mask and did not find significant difference in the etching. This fact suggests that the taper etching is mostly due to the physical shielding of ions instead of deflection of ion flux by disturbing the electric field distribution near the sample surface.

The waveguides on our test samples had inverted ridges. For channel waveguides with ridges on the top, selectivity of the etching can be used to avoid a removal of the ridge. Selectivity is adjustable via changing RIE parameters . An alternative method to protect the ridge is to pattern a photoresist line with the same width as the ridge on the upper cladding above the ridge waveguide before taper etching.

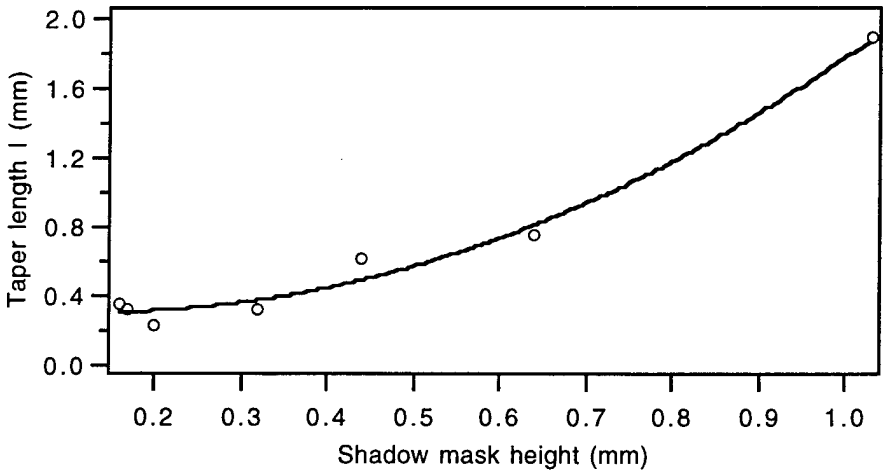

Fig. 7 Taper length as a function of shadow mask height.

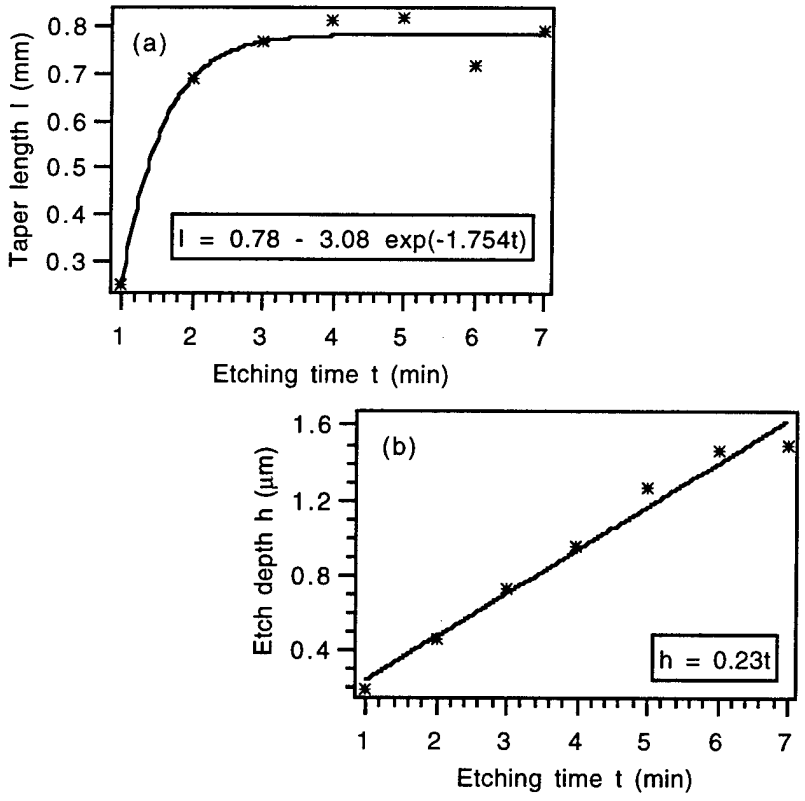

Fig. 8 (a) Taper length and (b) etch depth as functions of etching time. Etching condition is 400 mTorr, 40 W and 50 sccm.

RIE with photoresist taper made by gray-scale mask photolithography

The second method for making the taper utilizes photolithography with a gray-scale mask , followed by RIE. A holographic plate is exposed with a computer generated pattern which has a linear change of gray levels. After developing and fixing, this holographic plate is used as a gray-scale photomask for patterning photoresist spun on the waveguide sample. The continuous change of exposure level in positive photoresist leads to a continuous change of photoresist thickness; therefore a vertical taper of photoresist is formed. This vertical taper is then transferred into the waveguide upper cladding using regular oxygen RIE. Fig 9 shows these processing steps and Fig. 10 are surface profiles of Hoechst AZ5214E photoresist and the final taper profile made in the waveguide upper cladding after RIE. A linear taper is made in our experiment, but other taper profiles can be obtained by changing the computer generated gray level pattern.

Both techniques described above worked well with our test samples. RIE with shadow mask is easy to realize, but since the tail of the S-shaped taper decays gradually, the surface ~1 mm beyond the taper may still have some residue slope. This unwanted surface slope can cause difficulty in thickness control. Photolithography with gray-scale mask requires more processing steps, but it provides better thickness uniformity after etching. In addition, the ability to control the taper profile with this method is useful in further optimization of the shape of the taper.

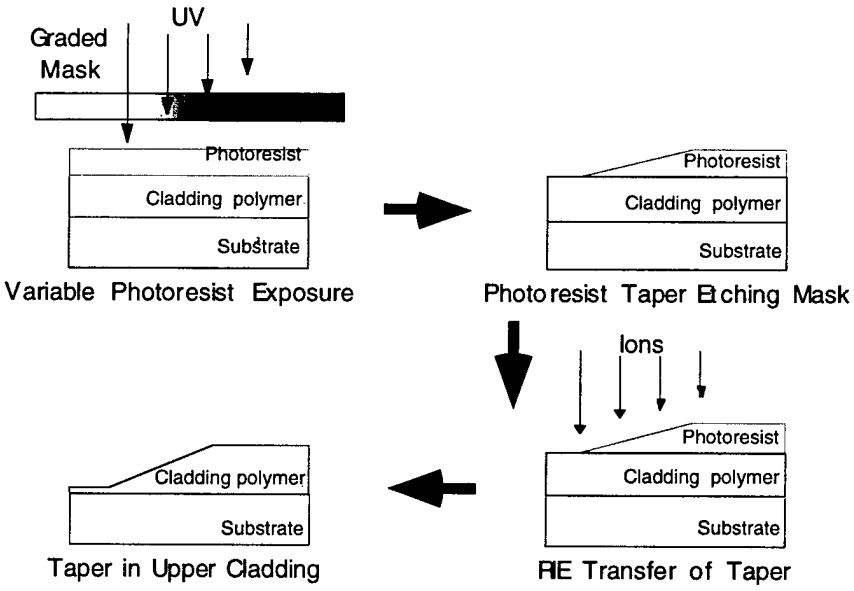

Fig. 9 Processing steps for vertical taper made by photolithography with a gray-scale mask.

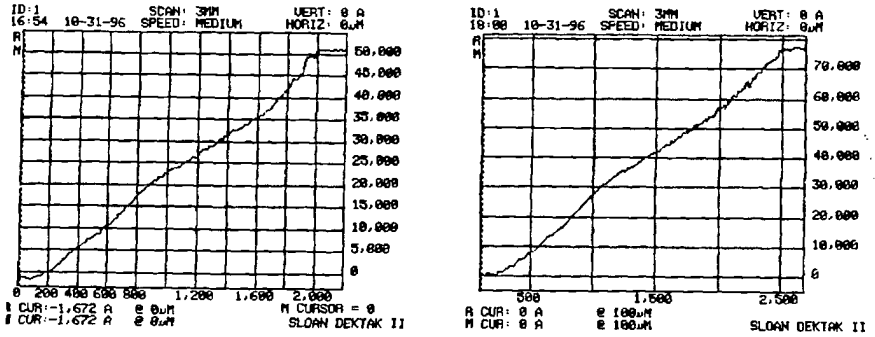

Taper in photo resist Taper in upper cladding

Fig. 10 Vertical tapers in photoresist and in cladding polymer. The horizontal scale is in µm and the vertical scale is in Å.

High index cladding The numerous varieties of polymers offer a wide range of refractive indices. A large choice of suitable new cladding materials is available. If the core layer is made of a chromophore containing polymer, for example an electrooptic polymer, the same polymer system with reduced chromophore number density can be used as new cladding material. For our test samples, Cargille Labs MeltMounts were chosen for the new cladding. MeltMounts are low Tg thermoplastic polymeric materials with low optical loss at the wavelength of 1.3 µm. They are solids at room temperature, but begin to liquefy if heated at above 70 °C. This property makes these materials attractive for experiment use. MeltMounts are available in several indices. By mixing two MeltMounts of different indices, one can get any index in between.

After the taper etching was completed, the waveguide samples were either diced with a wafer saw or cleaved to get a good endface for fiber coupling. A 5 mm wide glass slip with two spacers attached on its bottom was placed on the sample, with its edge aligned to the tapered end, and held in place with UV curable epoxy. The thickness of the spacers was 0.2 mm. They determined the thickness of the new cladding layer. Melt MeltMount was dropped on the inside edge of the glass slip and it flowed in the gap between the glass slip and the sample until it reached the end of the sample. A vertical surface was formed at the end of the gap due to surface tension. The shape of this endface remained unchanged after MeltMount solidified. Fig. 11 and Fig. 12 are an illustration of the finished sample and a microscopic photograph of the endface, respectively.

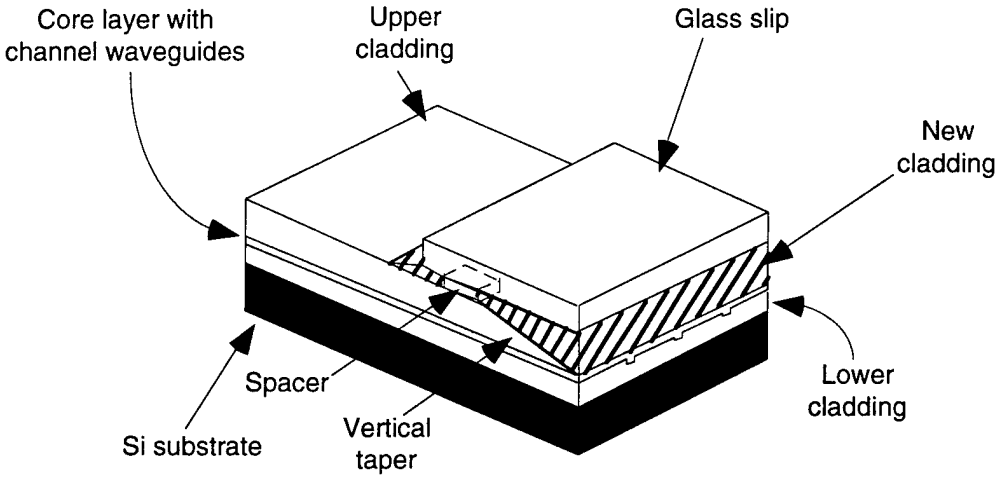

Fig. 11 The structure of the finished taper mode size transformer.

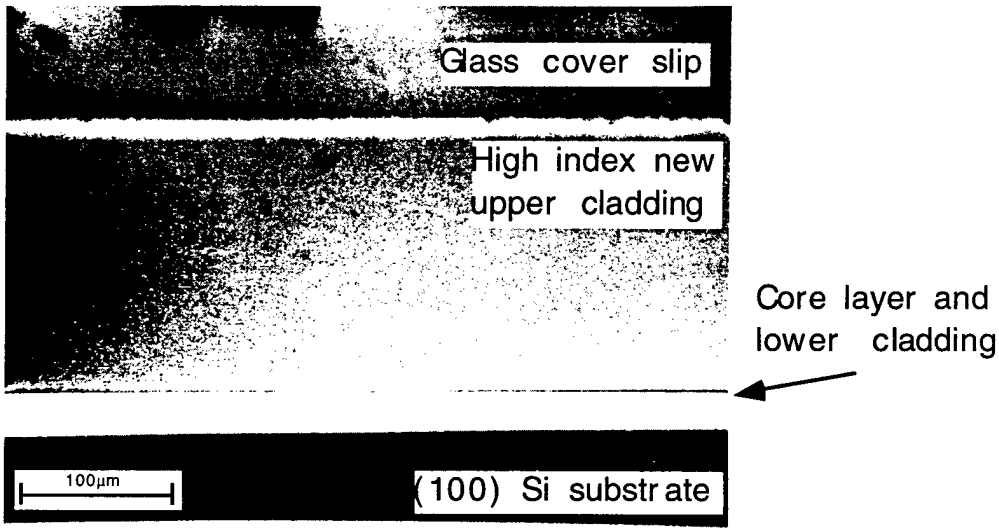

Fig. 12 The endface of a finished test sample.

C. Expermental Results

The test samples are inverted ridge waveguides with mode size transformer fabricated at one end. The cross section of the waveguide prior to taper etching is given in Fig. 13. The polymers used for upper cladding and core are Epoxylite 9653-2 resin and PU-DR19[20] , respectively. Both materials are thermoset. A vertical taper 0.5-2 mm long is etched in the upper cladding and slightly into the core layer. The final thickness of the core layer is 1.2±0.2 μm. Both taper etching techniques were used on these samples. The refractive index of the new cladding is 1.6265 at the wavelength of 1.3 μm. In order to observe the waveguide mode at various positions in the taper, some samples had taper aligned at an angle with the end of the sample. In this way, the

outputs from the different channel waveguides show the mode at different points in the taper, as shown in Fig. 14.

Fig. 15 is a schematic diagram of the test setup. A 1.3 μm pigtailed laser diode with an output power of 1.5 mW was used as light source. The measured mode size of the fiber is 10.5 μm. The out-coupling was made with a 60^X/0.8 NA microscope objective lens. A screen and an infrared camera were used to observe the imaged near field pattern of the output mode. For optical power measurements, the output light was focused on a photodetector. The fiber, the waveguide sample and the objective lens were mounted on alignment stages equipped with piezoelectric actuators. Alignment and data acquisition were controlled by a computer.

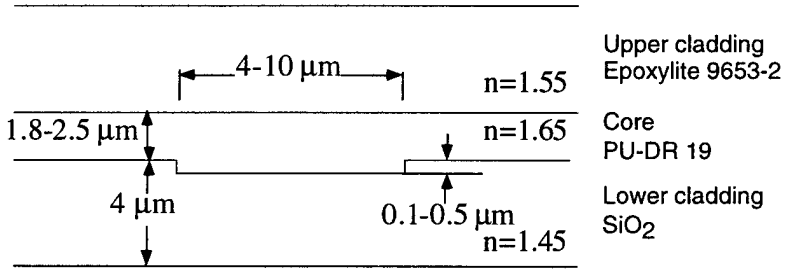

Fig. 13 The channel waveguide geometry of test samples.

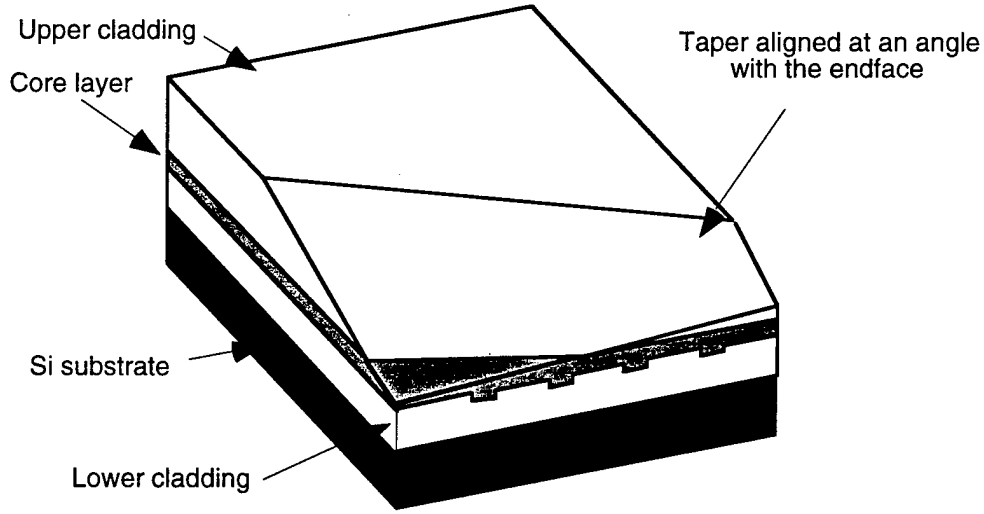

Fig. 14 The structure of a test sample made for observation of mode expansion in the taper. The taper is aligned at an angle with respect to the end of the chip. High index new cladding is not shown.

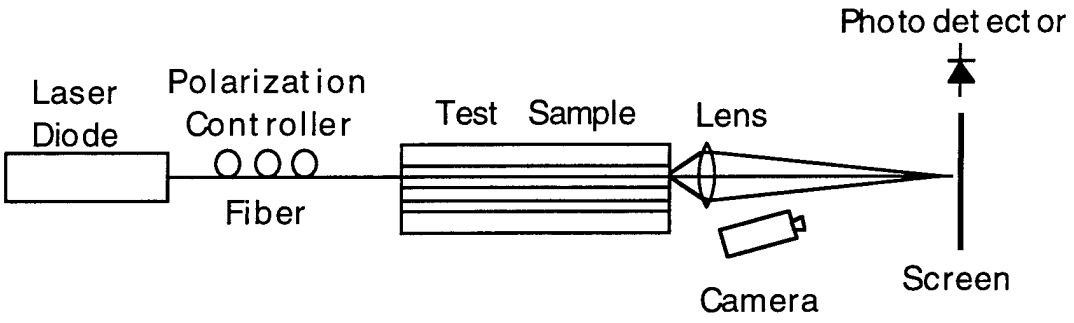

Fig. 15 Waveguide test setup.

Fig. 16 are pictures of modes in different positions of the taper. The mode size transformation in the taper is clearly seen. Mode expansion is also verified by an increase of fiber misalignment tolerance at the tapered end of the sample, as shown in Fig. 17.

The improvement of coupling efficiency is obtained by comparing the insertion loss of the sample when the fiber is coupled to the tapered end and the insertion loss when the fiber is coupled to the non-tapered end. Fig. 18 is a typical result from this measurement. The reduction of coupling loss for different waveguide widths and two polarizations is summarized in Table 1. These values are repeatable from several samples. The fact that the improvement of coupling is independent of waveguide width indicates that the lateral confinement of waveguides is not affected by the vertical expansion of mode. The experimental results also demonstrated that the performance of this taper mode size transformer is polarization insensitive, a very desirable property for many integrated optics devices.

Fig. 16 Photographs of expanded modes.

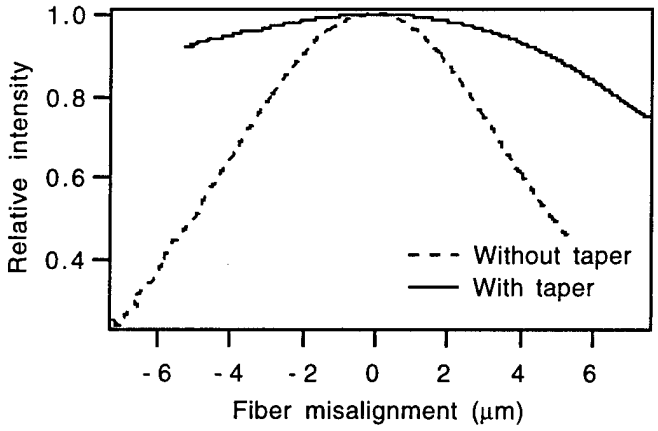

Fig. 17 Comparison of fiber misalignment in the vertical direction with and without taper mode size transformer.

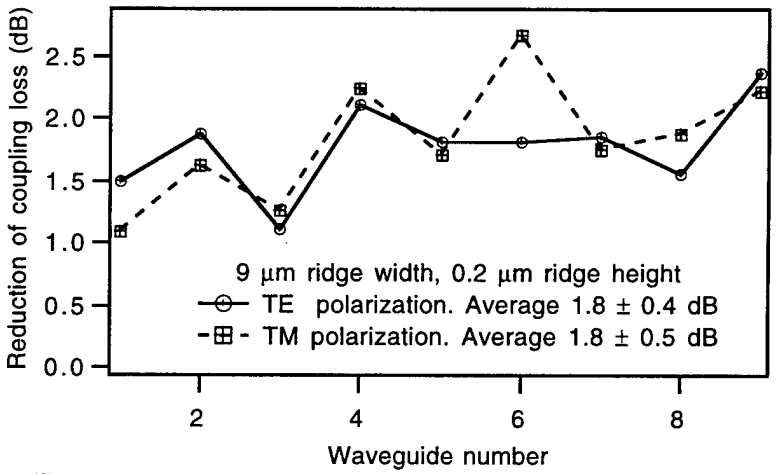

Fig. 18 Improvement of fiber coupling from a set of 9 waveguides.

Table 1 Improvement of fiber coupling efficiency, measured from of 8-9 waveguides of each width.

Polarization	Waveguide width (μm)			
	4	5	6	9
TE	1.8±0.3	1.7±0.3	1.4±0.4	1.8±0.4
TM	2.2±0.1	1.9±0.3	2.1±0.3	1.8±0.5

The lowest insertion loss for one taper section and propagation through 1 cm of waveguide is 4.4 dB without index matching at waveguide input and output facets. However, this value is not as low as theoretical prediction. Taking into account the calculated 1.6 dB coupling loss due to mode mismatch, the 1.4 dB/cm waveguide propagation loss obtained from previous cut-back

measurement, and 0.5 dB due to facet reflections, there is about 1 dB of unaccounted loss. Facet imperfection and scattering loss due to the roughness of the etched surface are the suspected sources of this excess loss. Inspection of the taper with microscope did reveal grain-like roughness on some tapers. This excess loss could be minimized by further improvement of fabrication techniques and optimization of the taper parameters.

III. Fast trimming of electro-optic polymer waveguide Y-branch by post-photobleaching for tuning the power splitting ratio

We present here, a simple, fast, and fault tolerant *in situ* trimming technique for the Y-branches of electro-optic polymer waveguides. Waveguide Y-branches are important basic building blocks in integrated optics and they are widely used in 3-dB couplers, power splitters, switches and Mach-Zehnder modulators. An ideal Y-branch 3-dB coupler divides the incoming power equally for the two branches with a unit power splitting ratio. In actual devices, however, the splitting ratio of a Y-branch always deviates from the ideal unity due to inevitable fabrication imperfections. Fig 1. shows the distribution of the error in the power splitting ratio of 100 Y-branches made in an electro-optic polymer by both low loss oxygen reactive ion etching and photobleaching. In the case of Mach-Zehnder modulators, a non-unity splitting ratio means a lower on-off ratio, smaller modulation depth, and higher noise level. An accurate splitting ratio currently relies on tight process control and results in lower yield and increased cost. A trimming method which can fine-tune the splitting ratio of an already fabricated Y-branch is very desirable. For this purpose, our novel trimming technique is effective for Y-branches of polymer strip waveguides made by the two major waveguide fabrication technologies; reactive ion etching (RIE) and photobleaching.

A. The Concept

The principle of this technique is based on the photobleaching of polymers. For polymers which contain photobleachable species, the refractive index of the polymer decreases upon irradiation with ultraviolet or visible light. Electro-optic (EO) polymers contain nonlinear chromophores, i.e., dye molecules, that give rise to both the electro-optic effect and photobleaching..

Fig. 2 shows the principle of our trimming technique. Suppose that the fabricated Y-branch sends more power into branch A than B. By photobleaching a small area at the A side of the waveguide immediately before the splitting point, the refractive index of that area is reduced. This localized index change shifts the mode peak away from side A, equivalent to a horizontal realignment of the waveguide mode before the splitting point. Less power is coupled into branch A, and more power is sent to branch B. The splitting ratio is, therefore, tuned towards unity without introducing substantial excess loss.

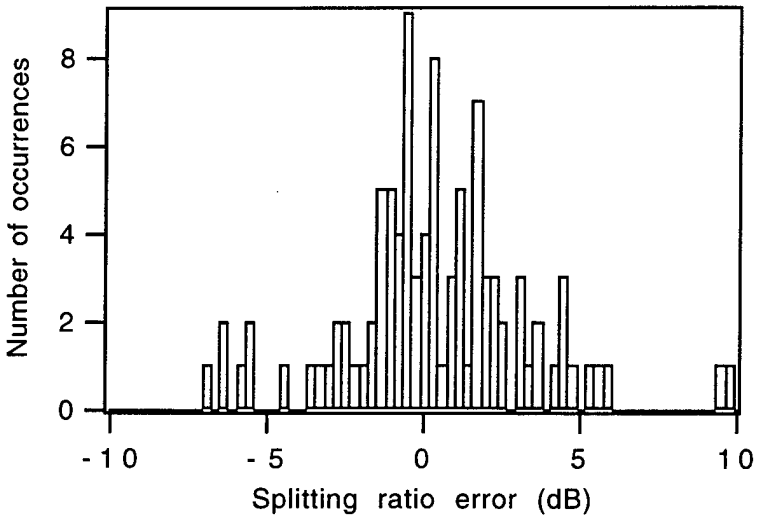

Fig. 1 The distribution of the power splitting ratio error of 100 Y-branches of EO polymer waveguides. 40 of them are made by oxygen reactive ion etching, and 60 of them are made by masked photobleaching.

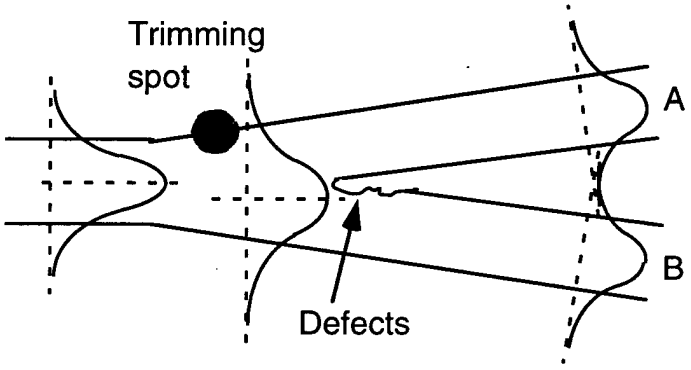

Fig. 2 The principle of the tuning of Y-branch power splitting ratio by focused photobleaching trimming.

B. Experiment

Test samples The trimming is performed on Y-branch samples that have finished all fabrication steps and with end faces prepared. The waveguide Y-branch samples used in the experiment are fabricated on silicon substrates. They have the same waveguide structure as the typical EO polymer devices. A 4 μm layer of Epoxylite® 9653-2 polyurethane or thermally grown SiO_2 is used as lower cladding. The waveguide core is a 1.5 μm thick layer of crosslinked PU-DR19 EO polymer. The absorption peak of the PU-DR19 polymer film is at 473 nm, very close to the trimming wavelength of 488 nm in the experiment. For

samples with etched waveguides, single mode strip waveguides with ribs 5-10 μm wide and 0.2-0.4 μm high are made in the core layer by photolithography and low loss oxygen plasma etching. For samples with photobleached channel waveguides, the Y-branches ware defined using a photolithographic mask aligner with a UV lamp peaked at 365 and 402 nm. The samples are exposed to the UV light under the same photomask used for patterning the RIE waveguide samples. The UV power is 5 mW/cm^2 and the exposure time is from 5 to 15 hours, for a total exposure energy density of 90-270 J/cm^2. The Y-branches have splitting angles from 2° to 3° in both cases. On top of the waveguide core layer, another layer of 5 μm polyurethane is spin-coated as upper cladding. The endfaces are prepared by cleaving at a low temperature of -16 °C. Low temperature cleaving eliminates the stretching and tearing of waveguide layers due to the increased rigidity and fragility of polymers and results in a clean break and a smooth endface.

Experimental setup The simple experimental setup is schematically shown in Fig. 3. The trimming uses the light from a 488 nm Ar^+ laser. The light is delivered by a multimode fiber. A binocular microscope is modified with a fiber fitting in one of the eyepiece bore to perform photobleaching. An eyepiece of the microscope is removed, and the output end of the fiber is placed in the image plane of the objective lens. The microscope objective reduces the output pattern of the fiber and projects a beam spot onto the sample. The size of the spot is determined by the fiber core size, the magnifying power of the microscope objective lens, and the axial position of the fiber tip. A spot size from 0.5 μm to >1 mm on the waveguide sample is obtainable. The position of the spot on the sample is observed through the other eyepiece or by a video camera on the microscope. Because the fiber tip is fixed to the microscope, its image always appears at the same place in the observation field of view when moving the microscope. This arrangement makes it very easy to position the beam spot to where trimming should be performed. Fig. 4 is a photograph of a Y-branch under trimming taken by the camera on the microscope. For monitoring the power splitting ratio, light from a pigtailed 1.3 μm laser diode is coupled to the waveguide by a single mode fiber. A polarization controller is used to selectively launch the TM or TE mode. The output powers of the two branches of the Y-branch are measured in real time during the trimming.

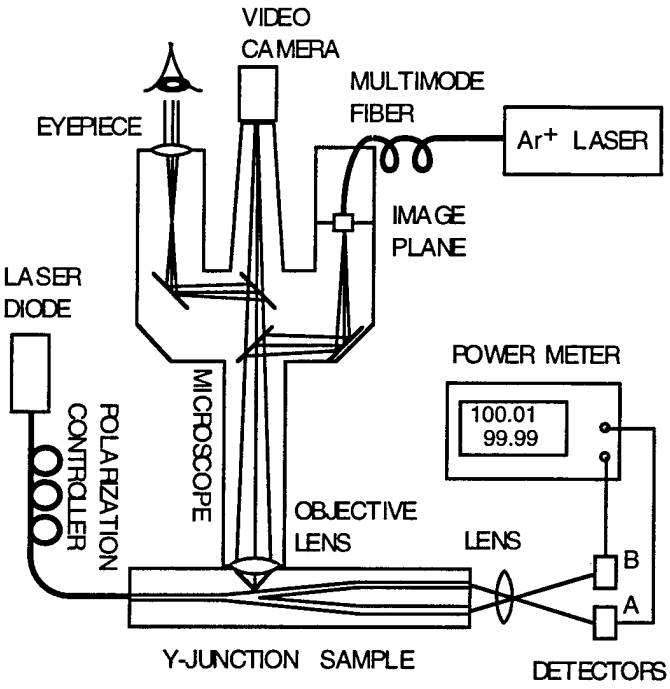

Fig. 3 Experimental setup for the trimming of waveguide Y-branch.

C. Trimming results

Fig. 5 shows the typical change of the output power of the two branches of a Y-branch under trimming. The branch which is being photobleached loses power due to a reduced refractive index, and the other branch gains power. The splitting ratio is, therefore, changed. Trimming the other branch causes the ratio to change in the opposite direction. This error correction capability makes this technique fault tolerant. A tunable range of the splitting ratio for the TE mode as wide as ±20% is achieved in our experiment. The trimming is effective for both the TE and TM modes, but the TE mode is found to have a tuning range approximately twice as large as that of the TM mode. This is because photobleaching produces a larger index change for the TE polarization than for the TM polarization. The change of the total output power from the two branches is less than 0.2 dB after repeated trimming of both branches. The excess loss is due to the scattering at the trimming point. After the trimming light is turned off, there is a fast partial recovery of the splitting ratio before it reaches a final stable value. This phenomenon is discussed in the following section and modeling the partial recovery is in progress. Over-trimming and multiple trimming sessions can be used to compensate the partial recovery and to reach the required splitting ratio, as demonstrated in Fig. 6. In the experiment, the power of the unpolarized trimming beam incident on the sample is only a few μW. Although the power is very low, it is focused on a small spot approximately 1 μm in diameter, producing a high power density and a short photobleaching time on the order of 10 seconds. Compared with the conventional masked

photobleaching which takes a few hours to complete, our focused photobleaching trimming is very rapid. From the index measurement at 1.064 μm and the extrapolated dispersion curve of this polymer, the index change of a thin film photobleached with the same energy density by a laser beam is found to be 0.025-0.03 at the wavelength of 1.3 μm. We have monitored the index change for over 3000 hours at room temperature and exposed to room light and observed no further change.

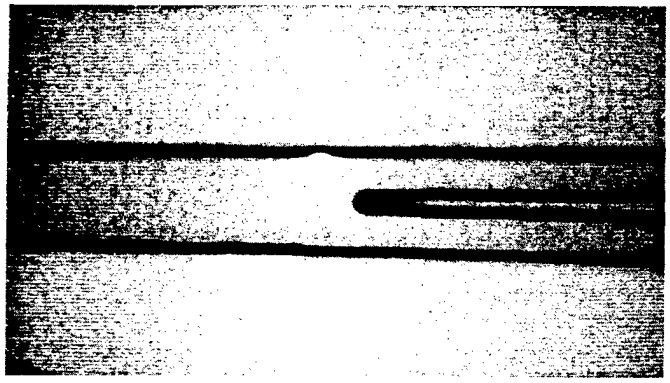

Fig. 4 A microscope picture of a Y-branch under trimming. The waveguide width is 6 μm.

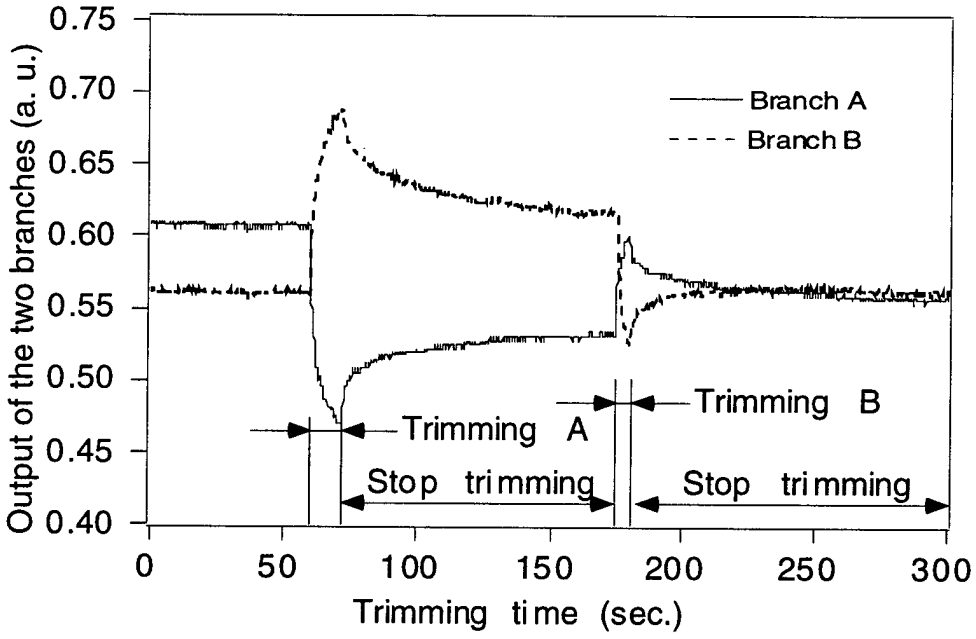

Fig. 5 The change of the output power of the two branches during laser trimming. A TE mode is launched in the waveguide. The trimming power is 6 μW, and the spot size is 2 μm. The power splitting ratio is tuned from 1.1 to 0.7 and finally to 0.99. The

excess loss due to trimming is 0.2 dB. Notice that a larger tuning range is achievable because the change of output power during trimming is not saturated.

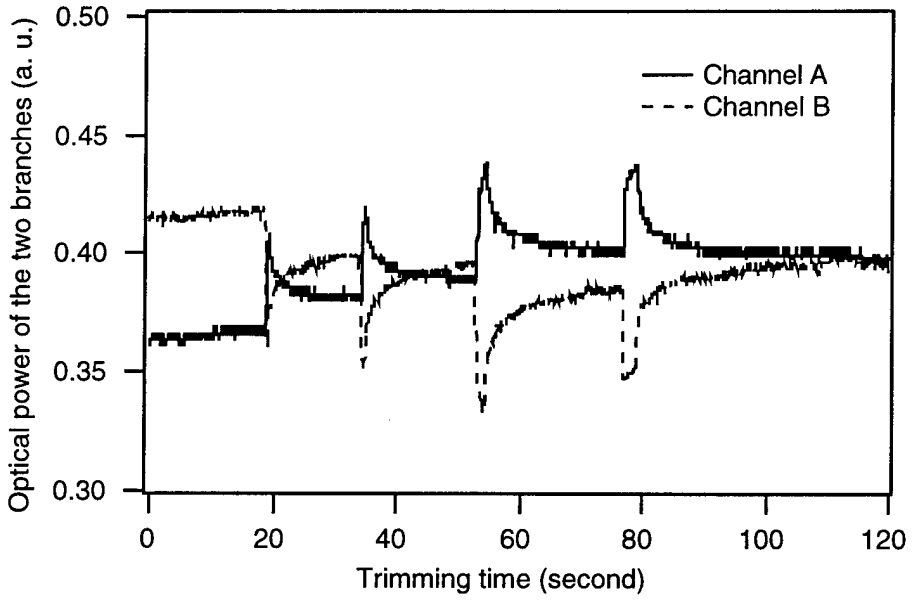

Fig. 6 Multiple trimming of the branch with higher output for equalizing the output powers.

D. Thermal and temporal stability of the trimming

Previous studies on the photobleaching have found three major processes contributing to the index change: trans-cis transformation of chromophores, sublimation of chromophores out of the material, and photodecomposition. The predominant bleaching process is an irreversible photodecomposition of the chromophores. Trans-cis transformation is reversible, and it has a typical relaxation time of a few seconds. This matches the speed of the partial recovery of the splitting ratio after trimming and, therefore, is believed to be a major source of this recovery. Possible heating in the trimming spot can also contribute to the partial recovery. The index changes due to sublimation and photodecomposition are irreversible and thus long-term stable. Since the chromophores in PU-DR19 are covalantly attached to the polymer network by two bonding sites, sublimation is minimal. The remaining index change after the initial relaxation is presumed to be due mostly to photodecomposition. Our Fourier transform infrared (FT-IR) and UV-VIS spectra of the photobleached films in Fig. 7 show diminished absorption bands belonging to the DR19 chromophores, a strong evidence of permanent chemical change. Breaking any of the chemical bonds destroys the chromophore and causes a change of the index of refraction. Because the TE and TM modes have different sensitivity to the trimming, light induced

orientation of chromophores may also exist as a second order effect. The angular alignment of the chromophores in thermally crosslinked PU-DR19 is found to be stable up to 90°C for 3000 hours. Therefore the trimmed splitting ratio due to the combined effect of photodecomposition and light induced orientation is expected to have good temporal stability.

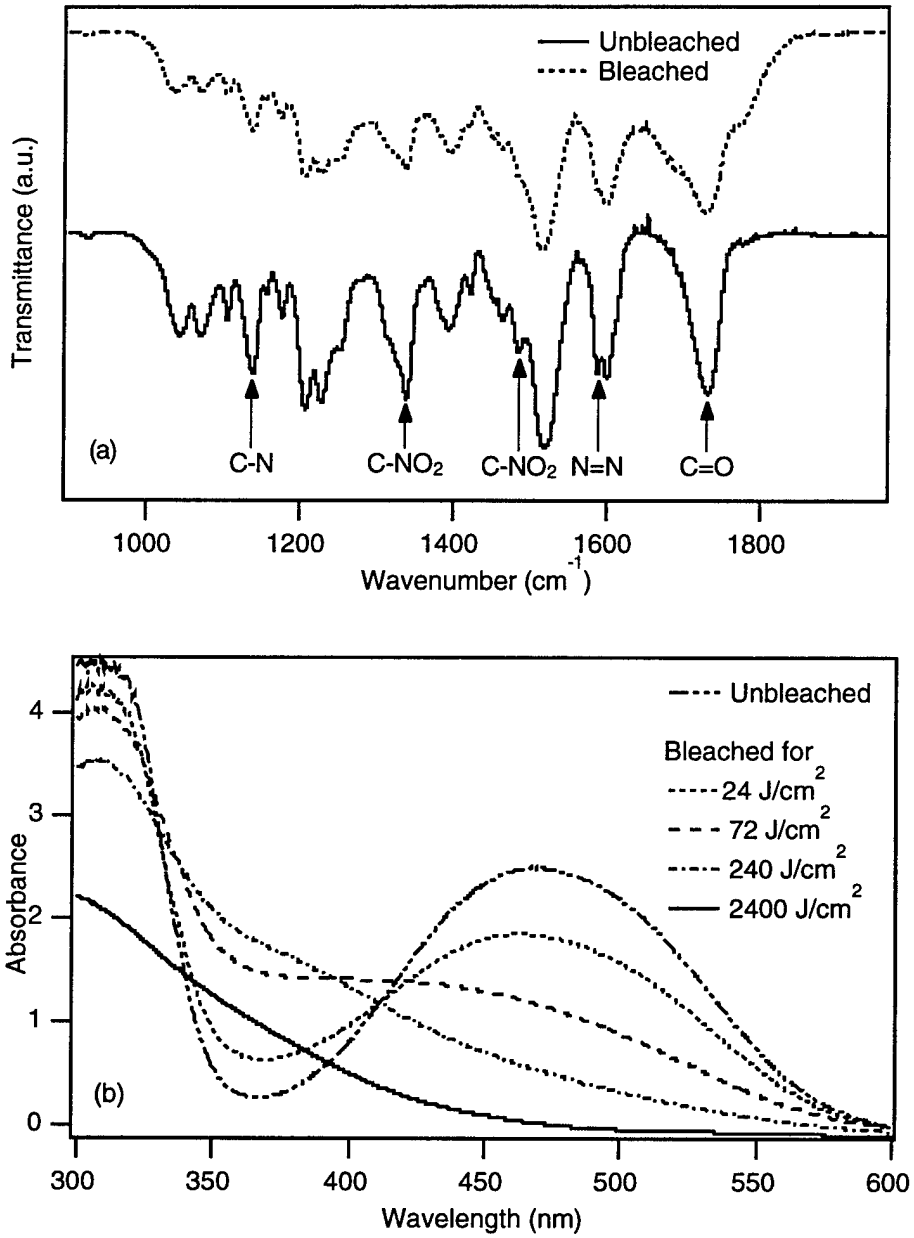

Fig. 7 Changes of the (a) FT-IR and (b) UV-VIS spectra of photobleached film and their corresponding chemical bonds. The nitrogen bonds belong to the DR 19 chromophore. Photobleaching was made with a 488 nm Ar^+ laser.

IV. Publications for the Three Year Program

1. "Photoinduced molecular alignment relaxation in poled electro-optic polymer thin films", Y. Shi, D. J. Olson, J. Bechtel, S. Kalluri, W. H. Steier, W. Wang, D. Chen, H. R. Fetterman, J. Appl. Phys., **88**, Febr. 19, 1996

2. "Simple two-slit interference electrooptic coefficients measurement technique and efficient coplanar electrode poling of polymer thin films", S. Kalluri, S. Garner, M. Ziari, W. H. Steier, Y. Shi, L. R. Dalton, Applied Physics Letters, 69, July 1, 1996.

3. "Optimized oxygen plasma etching of polyurethane based electrooptic polymers for low loss optical waveguide fabrication", A. Chen, K. Kaviani, A. Remple, S. Kalluri, W. H. Steier, Y. Shi, Z. Liang, L. R. Dalton, submitted to Journal of the Electrochemical Society.

4. "Processible and thermally stable heterocyclic polymers for second-order nonlinear optical studies", Z. Liang, Z. Yang, B. Wu, L. R. Dalton, S. Garner, S. Kalluri, A. Chen, W. H. Steier accepted for publication in Chemistry of Materials.

5. "Wavelength Dependent Photoinduced Depoling in Poled NLO Polymer Thin Films", Y. Shi, D. J. Olson, J. Bechtel, S. Kalluri, S. Garner, W. H. Steier, SPIE Proceedings, Vol. **2527** (1995).

6. "Novel electro-optic measurement technique for coplanar electrode-poled polymers", M. Ziari, S. Kalluri, S. Garner, W. H. Steier, Z. Liang, L. R. Dalton, Y. Shi, SPIE Proceedings, Vol. 2527 (1995).

7. "Integration of Polymer Electro-optic Devices on Nonplanar Silicon Integrated Circuits" S. Kalluri, M. Ziari, A. Chen, W. H. Steier, Z. Liang, L. R. Dalton, SPIE Proceedings, Vol. **2527** (1995).

8. "Monolithic Integration of Waveguide Polymer Electrooptic Modulators on VLSI Circuitry", S. Kalluri, M. Ziari, A. Chen, V. Chuyanov, W. H. Steier, D. Chen, B. Jalali, H. Fetterman, and L. R. Dalton, Phot. Tech. Lett., Vol.8, May, 1996.

9. "Synthesis and Characterization of 1,3 - Bis(dicyanamethylene) Indane Based Second Harmonic Order NLO Materials", S. Sun, C. Zhang, L. R. Dalton, S. M. Garner, A. Chen, W. H. Steier, Matr. Res. Soc. Sym. Proc. **413**, p 263-268 (1996) also accepted for publication in Chem. of Matr.

10. "Fabrication and Characterization of High Speed Polyurethane-Disperse Red 19 Integrated Electro-optic Modulators for Analog System Applications", Y. Shi, W. Wang, J. H. Bechtel, A. Chen, S. Garner, S. Kalluri, W. H. Steier, D. Chen, H. R. Fetterman, L. R. Dalton, Accepted for publication in IEEE J. Quant. Electr.

11. "Translating microscopic optical nonlinearity to macroscopic optical nonlinearity: The role of chromophore-chromophore electrostatic interactions" A. Harper, M. He, F. Wang, J. Chen, J. Zhu, S. Sun , L. R. Dalton, A. Chen, S. Garner, A. Yacoubian, W. H. Steier, D. Chen, H, R, Fetterman, Accepted for publication in J. Optical Society Amer., B.

12. "Trimming of Polymer Waveguide Y-junctions by Rapid Photobleaching for Tuning the Power Splitting Ratio", A. Chen, V. Chuyanov, F. I. Marti-Carrera,

S. Garner, W. H. Steier, S. S. H. Mao, Y. Ra, L. R. Dalton, accepted for publication in Photonic Technology Letters
13. "Progress Towards Device-Quality Second-Order NLO Materials: 1. Influence of Composition and Processing Conditions of Chromophore-Containing Polyurethane Networks on Nonlinearity, Temporal Stability, and Optical Loss", S. S. H. Mao, Y. Ra, L. Guo, C. Zhang, L. R. Dalton, A. Chen, SA. Garner, W. H. Steier, Submitted to Chemistry of Materials
14. "A Heterocylic Polymer with Thermostable Second Order Optical Nonlinearity", Z. Liang, L. R. Dalton, S. Garner, S. Kalluri, A. Chen, W. H. Steier, Chem. Matr. **7**, 1756-1758 (1995)
15. "Mode transformer with a teper section in polymer waveguide devices for efficient fiber coupling" AS. Chen, V. Chuyanov, F. I. Marti-Carrera, S. Garner, W. H. Steier, J. Wang, S. Sun, L. R. Dalton, SPIE Photonics West, paper 3005-11, Febr. 1997
16. "High-bandwidth polymer modulators". D. Chen, H. R. Fetterman, A. Chen, W. H. Steier, L. R. Dalton, W. Wang, Y. Shi,SPIE Photonics West, paper 3006-38, Febr. 1997
17. "Fast triming of electro-optic polymer waveguide Y-branch by post photobleaching to adjust the power splitting ratio", A. Chen, V. Chuyanov, F. I. Marti-Carrera, s. Garner, W. H. Steier, L. R. Dalton, SPIE, San Diego, CA August 1997.
18. "Preparation and NLO properties of 1,3-bis(dicyanomethylidene)indane(BDMI) based chromophores in PMMA thin films" S. Sun, L. R. Dalton, S. Garner, W. H. Steier, Am . Chem. Soc. Meeting, San Fransico, 1997, Polymer Reprints Vol. 38, 1997
19. "High Band Width Polymer Modulators" (Invited), D. Chen, H. R. Fetterman, A. Chen, W. H. Steier, L. R. Dalton, W. Wang, Y. Shi, LEOS'96, Nov. 18-21, 1996, Paper MI 1.
20. "Integration of Polymer Waveguide Electrooptic Modulators and VLSI Electronics using Standard Lithographic Fabrication Techniques", S. Kalluri, M. Ziari, W. H. Steier, L. R. Dalton, Z. Karim, Paper WL62, OFC '97, Dallas, TX, Febr., 1997.
21. "Progress towards the translation of large microscopic nonlinearities into large macroscopic nonlinearities in high $\mu\beta$ materials", J. Zhu, M. He, A, Harper, S. Sun, L. R. Dalton, S. Garner, Polymer Reprints Vol. 38, 1997.
22. "Design and synthesis of a perfluoroalkyldicyanovinyl-based NLO material for electro-optic applications" F. Wang, A. Harper, M. He, L. R. Dalton, S. Garner, Polymer Reprints Vol. 38, 1997.
23. "Novel electro-optic measurement technique for coplanar electrode-poled polymers", M. Ziari, S. Kalluri, S. Garner, W. H. Steier, Z. Liang, L. R. Dalton, Y. Shi,SPIE NonLinear Optical Properties of Organic Materials VIII, San Diego, CA July 1995.
24. "Integration of Polymer Electro-optic Devices on Nonplanar Silicon Integrated Circuits" S. Kalluri, M. Ziari, A. Chen, W. H. Steier, Z. Liang, L. R. Dalton, SPIE NonLinear Optical Properties of Organic Materials VIII, San Diego, CA July 1995.